DASA-11.026

R 264

Technical Report

COMPUTER CALCULATION OF DOSE RATES IN TWO-LEGGED DUCTS USING THE ALBEDO CONCEPT

24 October 1963

U. S. NAVAL CIVIL ENGINEERING LABORATORY

Port Hueneme, California

COMPUTER CALCULATION OF DOSE RATES IN TWO-LEGGED DUCTS USING THE ALBEDO CONCEPT

DASA-11.026

Y-F011-05-329

Type C

by

J. M. Chapman

ABSTRACT

This report gives the results of calculations of gamma-ray dose rates in two-legged rectangular concrete ducts. The calculations were performed on an IBM 1620. They are based on the differential dose albedo and include multiple scattering effects. The results of the calculations are compared with experimental data for ducts whose widths vary from 11 inches to 6 feet, using Co-60, Cs-137, Au-198, and Na-24 gamma-ray sources. The calculated dose rates agree to within ±30 percent for all ducts and all sources, except for small ducts with Cs-137 sources, ducts with very short first legs ($L_1/W \leq 1.33$), and for Au-198 sources.

INTRODUCTION

The ability to calculate dose rates in two-legged ducts would be of great assistance to engineers designing shelter entranceways. If the calculations were based on basic scattering principles and were verified experimentally, it would give great insight into the phenomena taking place in radiation attenuation in a duct.

The LeDoux-Chilton method[1] was developed on the albedo concept, where the dose contributions from the different scattering areas in a duct were calculated using the differential dose albedo. However, at the time of the development of this computational technique, values for differential dose albedo were not known. Values for differential dose albedos for various gamma-ray energies and entrance and exit angles have since been calculated by Technical Operations, using the Monte Carlo method.[2] Using the Technical Operations data, Chilton and Huddleston[3] developed a semiempirical equation from which the differential dose albedo can be calculated for any energy and any entrance and exit angle. Ingold[4] used this equation to calculate build-up in the first leg and obtained good agreement with experimental results.

With an equation for albedo, and the equations for corner lip inscattering and penetration effects, it became feasible to calculate theoretical dose rates in concrete ducts with an electronic computer. For these calculations, four programs were written for the IBM 1620: (1) a program which performs the calculations devised in Reference 1, (2) a program which uses small incremental areas for calculating the dose rates from the primary scattering areas, (3) a program which calculates the dose rates from multiple scattering in the first and second legs of the duct, and (4) a program which calculates the dose rates due to multiple scattering of gamma rays that are deflected (inscattered) by the corner lip. These programs therefore include all processes which involve one or two interactions; that is: one backscatter, one inscatter, one backscatter and one penetration, two backscatters, and one backscatter and one inscatter.

In the study that follows, the method developed for calculating the differential dose albedo is presented, then the four computer programs are outlined, and the results of the calculations are compared with experimental measurements. The study was sponsored by the Defense Atomic Support Agency through the Bureau of Yards and Docks.

CALCULATION OF DIFFERENTIAL DOSE ALBEDO

The dose rate at the detector from the scattering area, A (Figure 1), is given by

$$D = \frac{D_0 a(E_0, \theta_0, \theta, \varphi) A \cos\theta_0}{r_1^2 r_2^2} \qquad (1)$$

where $a(E_0, \theta_0, \theta, \varphi)$ = the differential dose albedo

A = the area of the scattering surface

D_0 = the dose rate at one unit length from the source

E_0 = the initial energy of the gamma rays from the source

Values for $a(E_0, \theta_0, \theta, \varphi)$ were calculated for various energies and entrance and exit angles by Technical Operations, Inc., using the Monte Carlo method.[2]

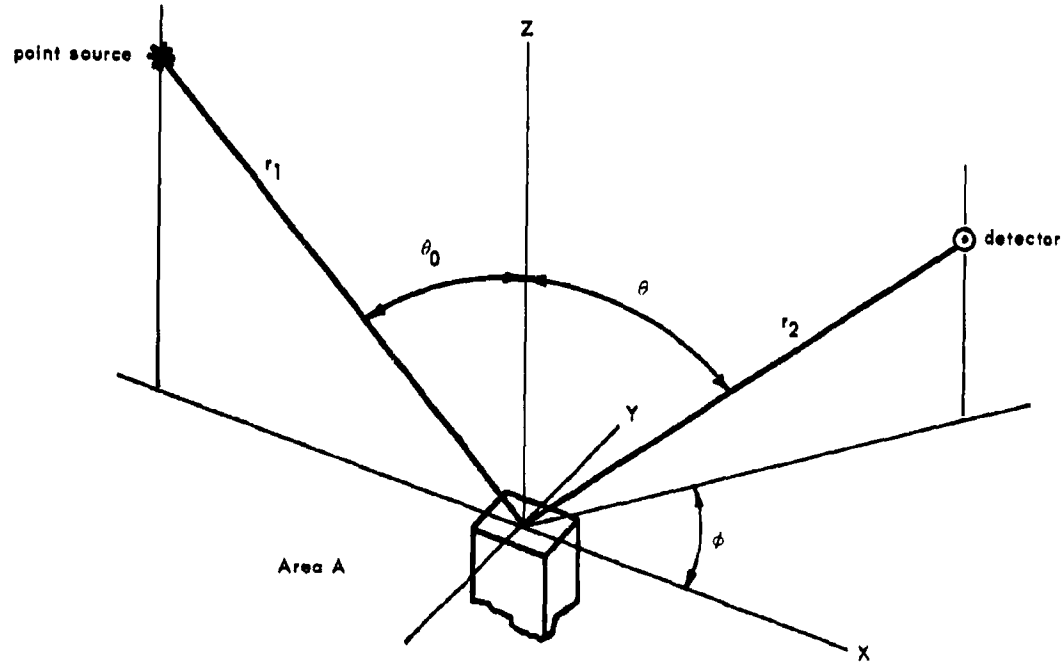

Figure 1. Scattering of gamma rays from surface.

The equation developed by Chilton and Huddleston [3] to express the albedo for a given energy is

$$a(E_0, \theta_0, \theta, \varphi) = \frac{C(E_0)\, K(\theta_s)\, 10^{26} + C'(E_0)}{1 + \dfrac{\cos\theta_0}{\cos\theta}} \qquad (2)$$

where $C(E_0)$ and $C'(E_0)$ are constants for a given energy, $K(\theta_s)$ is the Klein-Nishina differential energy scattering coefficient, and θ_s is the angle through which the radiation is scattered and is given by

$$\cos\theta_s = \sin\theta_0 \sin\theta \cos\varphi - \cos\theta_0 \cos\theta$$

Chilton and Huddleston found $C(E_0)$ and $C'(E_0)$ by the least-squares fit of the Technical Operations data by both a nonweighted fit and a weighted fit. The values of C and C' found by the weighted fit are plotted in Figure 2. For calculation on the computer, the curves of Figure 2 were fitted by the equations:

$$C = \exp[-2.921 + 0.6805 \ln E + 0.0111 (\ln E)^2 - 0.04131 (\ln E)^3] \qquad (3)$$

$$C' = \exp[-5.89 + 0.275 (E - 3.25)^2] \qquad 0.1\,\text{mev} \leq E \leq 1\,\text{mev}$$

$$C' = \exp[-4.86 + 0.36 (E - 2)^2] \qquad 1\,\text{mev} \leq E \leq 2\,\text{mev} \qquad (4)$$

$$C' = \exp[-4.83 - 0.013E] \qquad 2\,\text{mev} < E \leq 10\,\text{mev}$$

PROGRAM 1. LEDOUX-CHILTON CALCULATIONS

For the calculations based on the LeDoux-Chilton method, [1] the duct is divided into the areas shown in Figure 3. A_1, A_2, and $A_3 + A_4$ are referred to as the primary scattering areas, those areas in view of both the source and the detector. A_5, A_6, A_7, and A_8 are those areas for which radiation must penetrate the corner lip before reaching the detector.

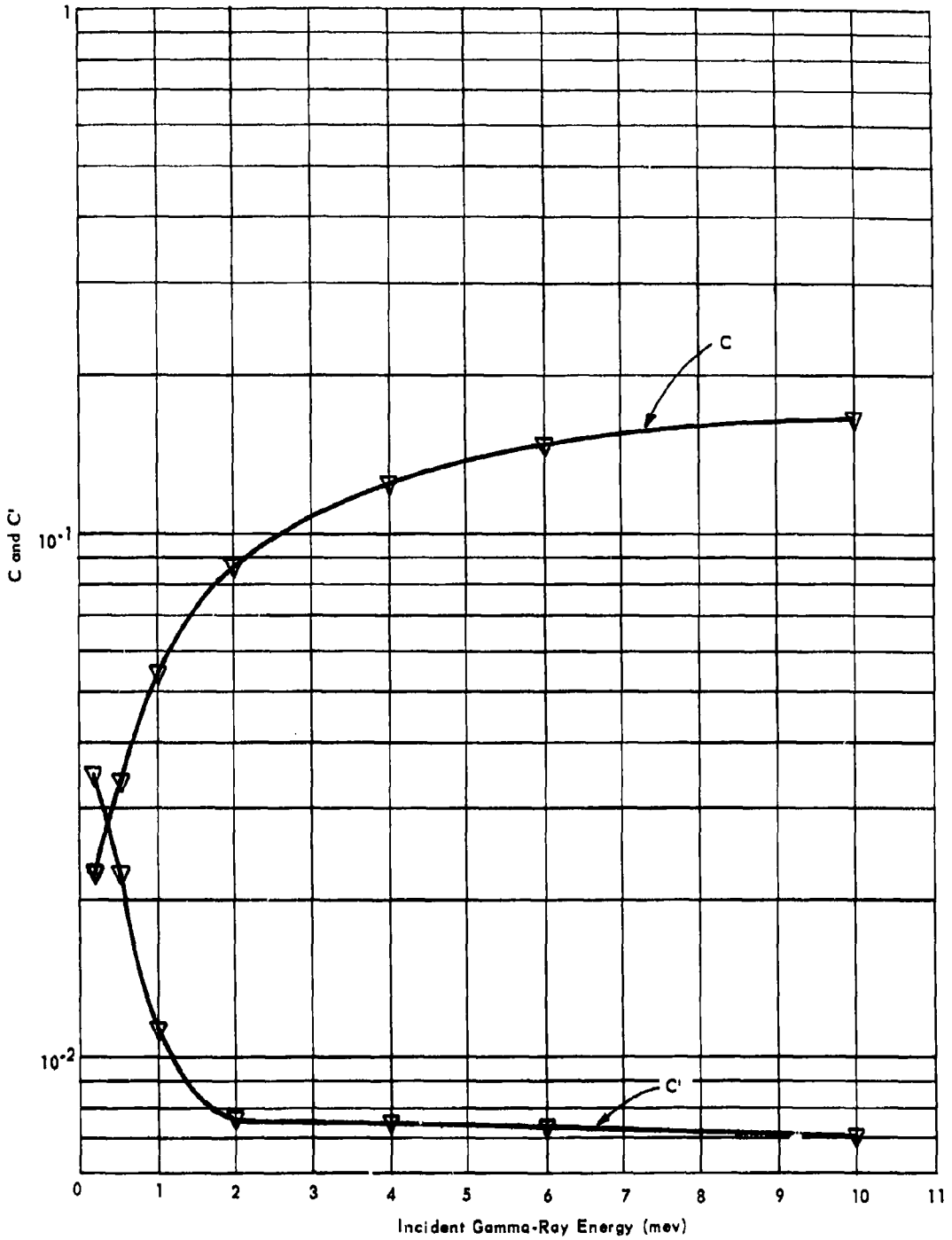

Figure 2. Parameters C and C' versus energy.

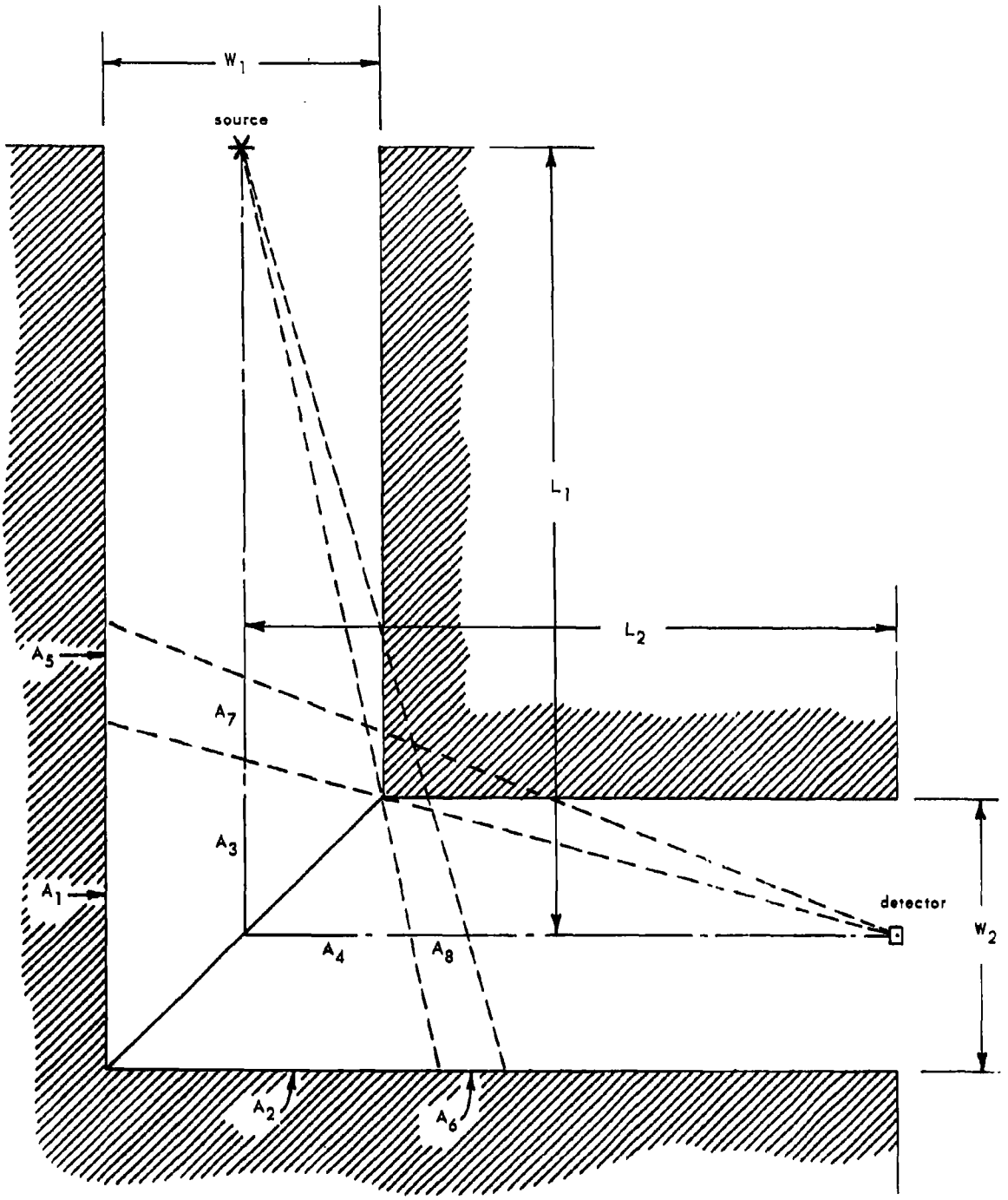

Figure 3. Duct geometry showing scattering areas.

The dose rate from any of the scattering areas is calculated from Equation 1, where r_1, r_2, θ_0, θ, and φ, shown in Figure 1, are measured at the center of the scattering area. The albedo, $a(E_0, \theta_0, \theta, \varphi)$, is calculated from Equation 2. $C(E_0)$ and $C'(E_0)$ in Equation 2 are calculated from Equations 3 and 4.

For areas A_5, A_6, A_7, and A_8 the size of the scattering area is found by assuming that all gamma rays traveling a distance of one mean free path or less through the corner lip reach the detector, and none traveling more than one mean free path reach the detector. The validity of this assumption is shown in Reference 1.

The mean free paths, or RL's (relaxation lengths), used are the reciprocals of the energy-absorption coefficients, as it is assumed that gamma rays scattered but not absorbed are scattered through a small angle. These mean free paths, found by taking the reciprocal of the energy-absorption coefficient for air given by Rockwell,[5] are plotted in Figure 4. For calculation on the computer, the curve of Figure 4 was fitted by the equations:

$$RL = 4.65E^{-0.24} \qquad E < 0.3\text{mev}$$

$$RL = 5.98 \qquad 0.3\text{mev} \leq E \leq 1.0\text{mev}$$

$$RL = 5.98E^{0.269} \qquad E > 1.0\text{mev}$$

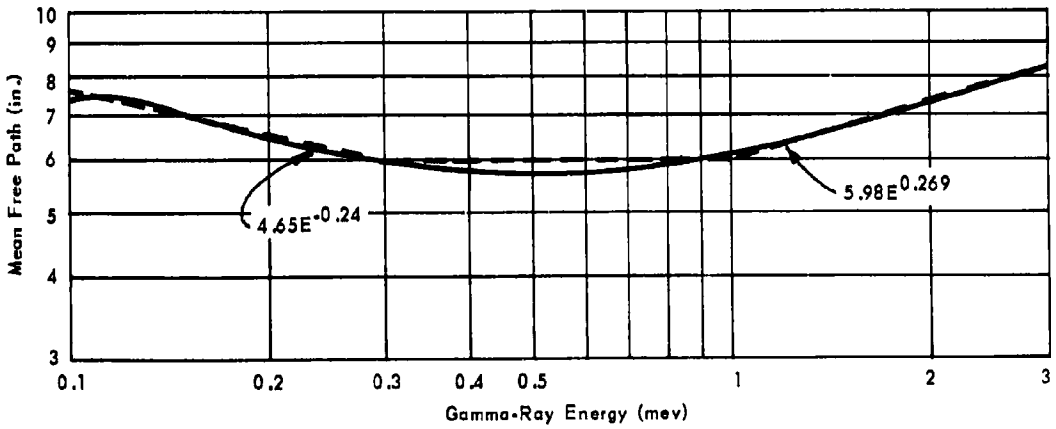

Figure 4. Energy-absorption mean free path for 145-lb/ft^3 air-equivalent concrete.

The remaining dose-rate contribution calculated with this program is that due to the inscatter of gamma rays at the corner lip, as shown in Figure 5. The equation developed in Reference 1 for this dose-rate contribution is

$$D = \frac{D_0 ZN\, K(\theta_s)\, H\, (RL)^2 \cos\theta_0 \cos\theta}{r_1^2 r_2^2}$$

where r_1, r_2, θ_0, θ, and θ_s are as shown in Figure 5 and are measured at the tip of the corner lip; H is the height of the duct; RL is the mean free path of the gamma rays in concrete and is given in Figure 4; and ZN is the number of electrons per unit volume and was calculated to be

$$ZN = 1.15 \times 10^{25} \text{ electrons/in.}^3$$

for 145-lb/ft^3 concrete.

The dose rates calculated with this program are about one-third of measured dose rates for small ducts and about one-half for large ducts. This would be expected from experimental evidence showing the importance of multiple scattering in a duct.[6,7]

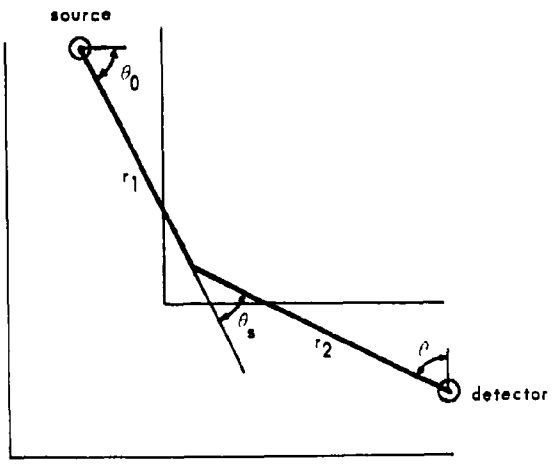

Figure 5. Geometry showing inscatter of gamma rays from corner lip.

PROGRAM 2. CALCULATION OF PRIMARY SCATTERING AREAS BY INCREMENTS

In the LeDoux-Chilton program, r_1, r_2, θ_0, θ, and φ were considered constant over each primary scattering area. This would not be a bad approximation for ducts with very long legs, but could give erroneous answers for ducts with legs of medium or short lengths. Therefore a program was written in which each primary scattering area is divided into small increments for its calculation. The corner is divided into the five areas shown in Figure 6. The ceiling (or floor) is divided into three areas for ease of calculation. Each area shown in Figure 6 is divided into several small increments. The dose rates for all the increments are calculated using Equation 1 and summed to give the dose for the primary scattering area under consideration. For each calculation, r_1, r_2, θ_0, θ, and φ are measured at the center of the incremental area.

The dose rate from a primary scattering area when calculated using small incremental areas was generally 50 percent higher than when calculated as one area, and was sometimes as much as 100 percent higher.

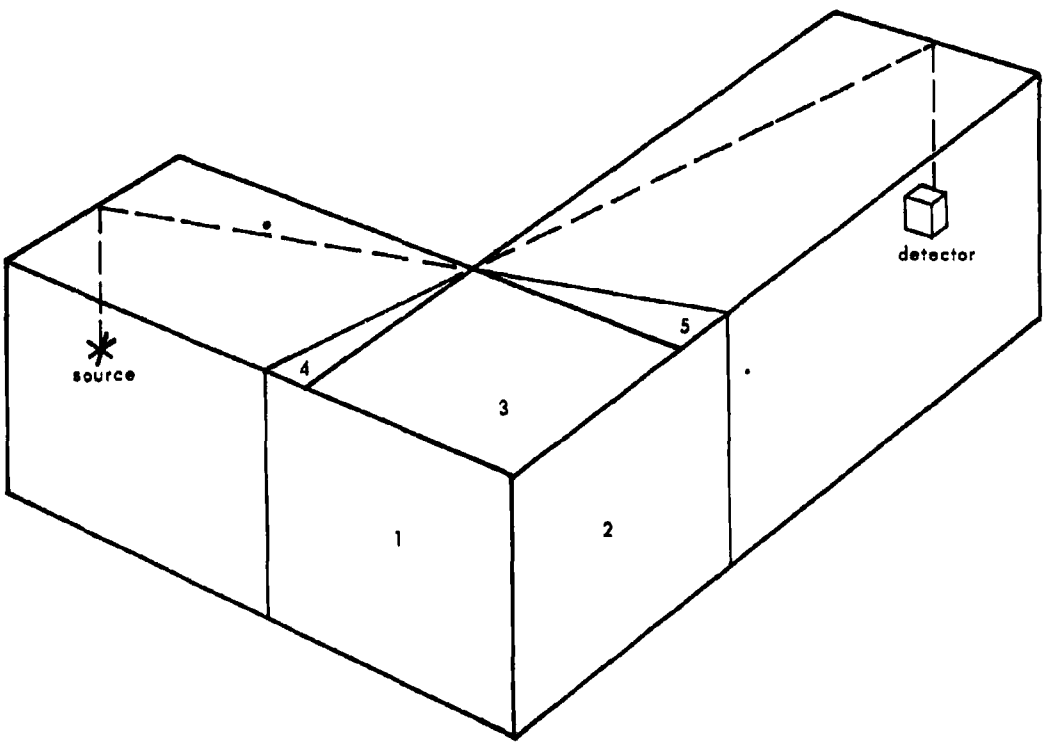

Figure 6. Division of primary scattering areas for calculation by incremental areas.

For the above results, each of the areas of Figure 6 was divided into 16 increments. It is felt that further division is undesirable, because it would greatly increase the running time on the computer. Also, finer divisions would probably give no increase in accuracy because of the tacit assumption that all gamma rays are backscattered at the interface. Actually, a backscattered gamma ray may emerge at distances of a mean free path or more from the point where it penetrated the wall of the duct.

PROGRAM 3. MULTIPLE SCATTERING CALCULATIONS

The dose-rate contribution from gamma rays which have been multiply scattered, that is which have been scattered from more than one scattering surface before reaching the detector, has been shown experimentally to be large. Therefore it is necessary to make some attempt to calculate this dose-rate contribution.

A program was written which calculates the dose rate from gamma rays that have been scattered from two scattering surfaces. The duct is divided into nine scattering surfaces, as shown in Figure 7. All possible combinations are taken for which a gamma ray from the source can scatter from one surface to another surface and then to the detector.

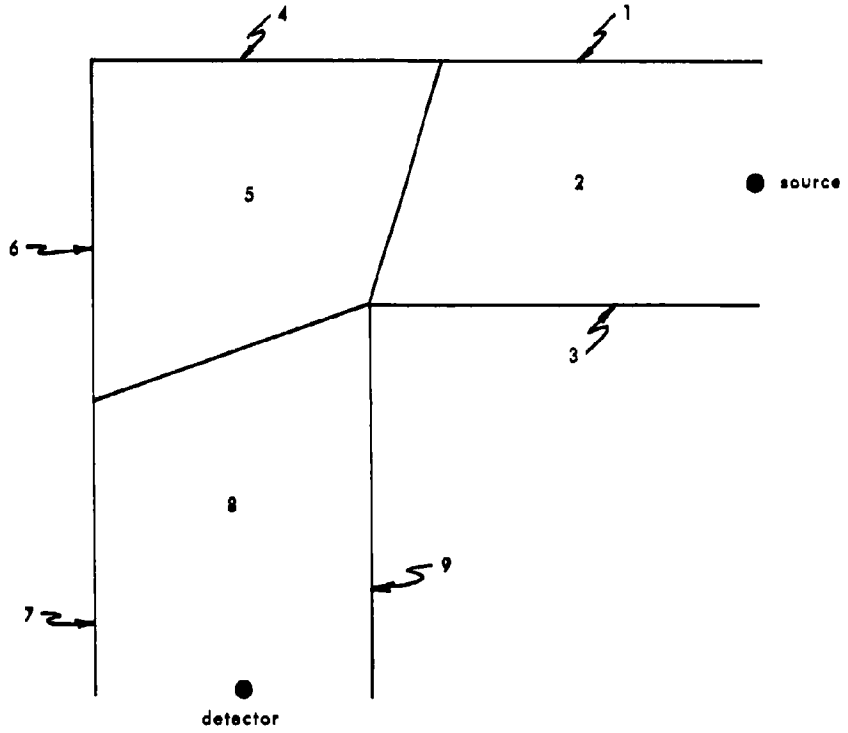

Figure 7. Scattering areas used in multiple scattering program. Areas 2, 5, and 8 are either ceiling or floor.

The dose rate at the center of the second area due to gamma rays from the source impinging on the first area is calculated. Then the dose rate at the detector due to the second surface and the previously calculated initial dose rate is computed. The energy of the gamma rays impinging on the second area is assumed to be the energy of a gamma ray having one Compton scatter at the center of the first area and going to the center of the second area.

The equations used for these calculations are then:

$$D = \frac{D_0 A_i A_j \cos\theta_{01} \cos\theta_{02} a_1 a_2}{r_1^2 r_2^2 r_3^2}$$

$$a_1 = \frac{C(E_0) K(\theta_{s1}) 10^{26} + C'(E_0)}{1 + \frac{\cos\theta_{01}}{\cos\theta_1}}$$

$$a_2 = \frac{C(E_s) K(\theta_{s2}) 10^{26} + C'(E_s)}{1 + \frac{\cos\theta_{02}}{\cos\theta_2}}$$

where A_i = the area of the first scattering surface

A_j = the area of the second scattering surface

E_s = the energy of a gamma ray undergoing one Compton scatter in going from the source to the center of A_i to the center of A_j

and r_1, r_2, r_3, θ_{01}, θ_{02}, θ_1, θ_2, φ_1, and φ_2 are as shown in Figure 8 for the case of $i = 3$ and $j = 5$. C and C' are calculated from Equations 3 and 4.

Three possible combinations of i's and j's were found to be too complicated to be put into this program. These are: $i = 1$ and $j = 8$, $i = 2$ and $j = 7$, and $i = 2$ and $j = 8$. Those combinations, believed to be small, were therefore neglected. This lack is offset by the assumptions that surface 8 is in view of all of surface 4, surface 6 is in view of all of surface 2, and surface 5 is in view of all of surface 2.

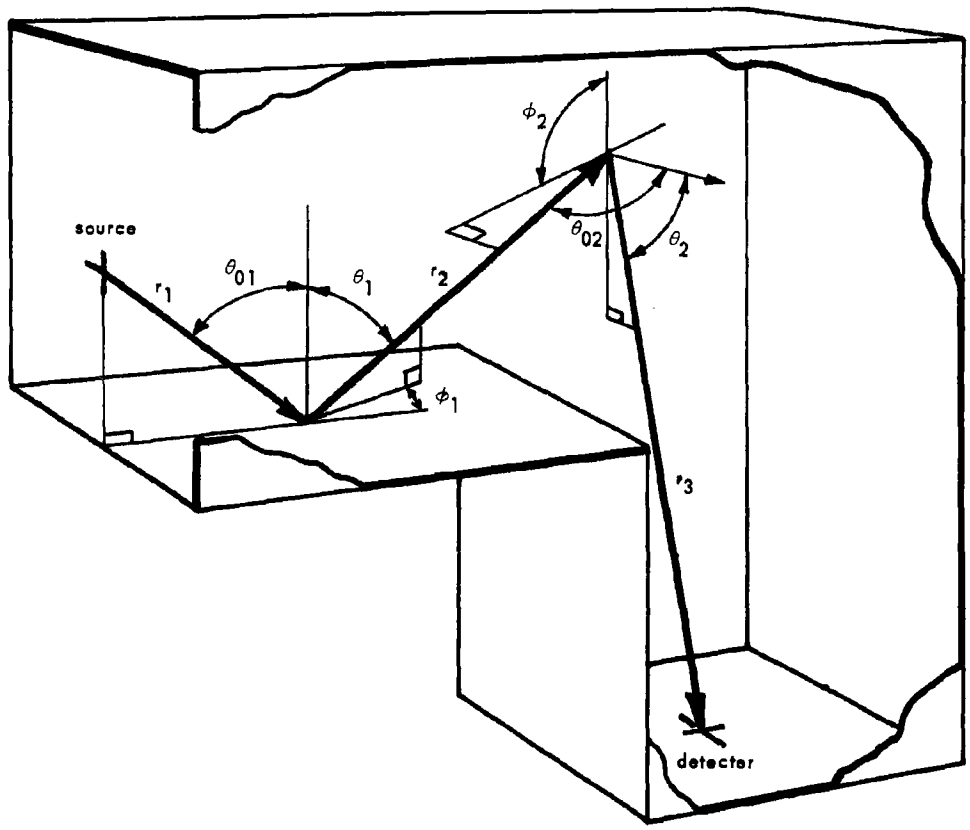

Figure 8. Geometry for multiple scattering for i = 3 and j = 5.

Special means were needed to calculate the combination i = 1 and j = 7. From Figure 9:

$$\frac{\overline{A_1A_7}}{H^2} = \int_{X_1}^{L_1 - \frac{W_2}{2}} y\,dx - X_2\left(L_1 - \frac{W_2}{2} - S\right)$$

$$= (S - X_1)\left(L_2 - \frac{W_1}{2} - X_2\right) + W_1W_2 \ln\left(\frac{L_1 - \frac{W_2}{2}}{S}\right)$$

$$- X_2\left(L_1 - \frac{W_2}{2} - S\right)$$

where $\overline{A_1A_7}$ is the effective product of those parts of A_1 and A_7 that are in view of each other. For this case r_1, r_2, r_3, θ_{01}, θ_{02}, θ_1, θ_2, θ_{s1}, and θ_{s2} are not measured at the center of A_1 and A_7, but as shown in Figure 9.

Dose rates calculated with the multiple scattering program generally represent a sizable portion of the total dose rate. For 6-foot-square ducts calculated, multiple scattering doses are about one-third of the total calculated dose rate.

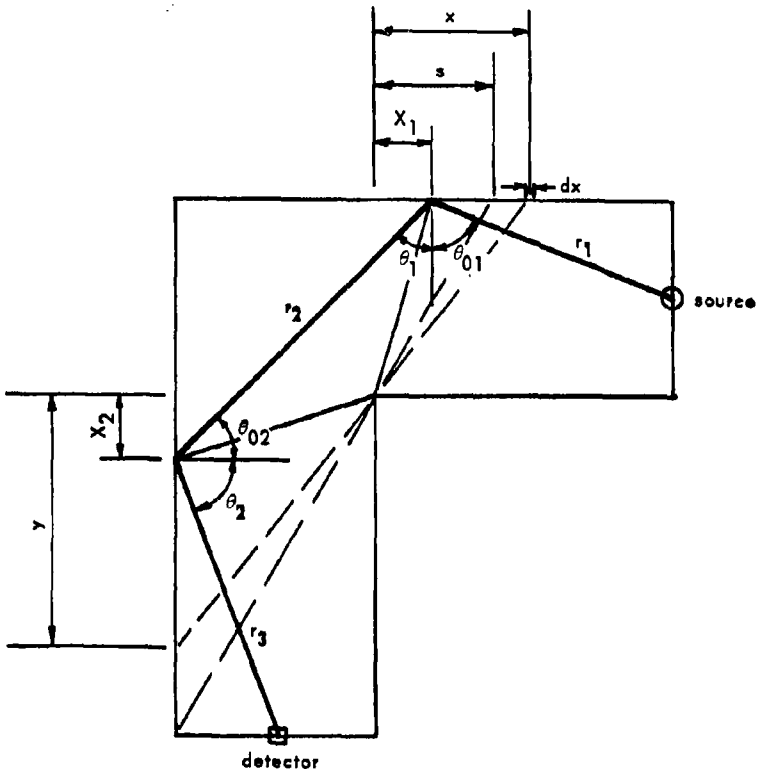

Figure 9. Geometry for calculating the 1-to-7 contribution.

PROGRAM 4. MULTIPLE CORNER INSCATTERING CALCULATIONS

The need for a more inclusive calculation of the corner lip effect was shown when the sum of the previous calculations (the corner lip penetration and inscatter from the LeDoux-Chilton program, the primary scattering surfaces from incremental areas, and the multiple scattering) gave fairly good results for large ducts, but very low results for small ducts. It was believed that the LeDoux-Chilton method of treating the corner lip was correct, but that an important contribution had not been

considered. The importance has already been shown for those dose contributions involving two processes; i.e., two backscatters, and a backscatter and a penetration of the corner lip (as for A_5, A_6, A_7, and A_8 in the LeDoux-Chilton analysis). Therefore, it was believed necessary to calculate those interactions involving backscatter from a surface and an inscatter from the corner lip.

The dose-rate contribution of the four cases involving these processes are calculated in this program. These four cases are shown in Figure 10. The first two cases involve a backscatter from a surface in the first leg to the corner lip and an inscatter from the corner lip to the detector. The other two cases involve an inscatter from the corner lip to a surface in the second leg and a backscatter from that surface to the detector.

The equations used for these calculations are, for Cases 1 and 2:

$$D = \frac{D_1 ZN K(E_1, \theta_{s2}) \cos\theta_1 \cos\theta_2 (RL_1)^2}{r_3^2}$$

where

$$D_1 = \frac{D_0 a A_1 \cos\theta_0}{r_1^2 r_2^2}$$

and for Cases 3 and 4:

$$D = \frac{D_1 a A_1 \cos\theta_0}{r_3^2}$$

where

$$D_1 = \frac{D_0 ZN K(E_0, \theta_{s1}) H \cos\theta_1 \cos\theta_2 (RL_0)^2}{r_1^2 r_2^2}$$

In the above equations:

a = the albedo, calculated by Equations 2, 3, and 4

A_i = the area of the scattering surface in the first leg

A_j = the area of the scattering surface in the second leg

D = the dose rate at the detector

D_0 = the dose rate at one unit length from the source

E_0 = the initial energy of gamma rays from the source

E_1 = the energy of a gamma ray scattered through θ_{s1}

$K(E, \theta_s)$ = the Klein-Nishina scattering coefficient

RL_0 = the mean free path for gamma rays of energy E_0

RL_1 = the mean free path for gamma rays of energy E_1

ZN = the number of electrons per unit volume in the corner lip

and r_1, r_2, r_3, θ_0, θ, θ_1, θ_2, θ_{s1}, θ_{s2}, and φ are as shown in Figure 10 and are measured at the center of the scattering area under consideration and at the tip of the corner lip.

These calculations give large dose-rate contributions, as will be seen in the following analysis of results. In general they account for about 50 percent of the total dose rate in small (11-inch-square) ducts and about 15 percent in large (6-foot-square) ducts. The contributions from Cases 3 and 4 are 5 to 10 times the contributions from Cases 1 and 2.

COMPARISON OF CALCULATIONS AND EXPERIMENTAL DATA

The results of all the calculations performed to date are given in Table I. As can be seen, the agreement between calculated values and measured values is normally better than ±30 percent. The exceptions to this agreement are the 12-inch duct with the Cs-137 source, ducts with very short first legs ($L_1/W = 1.33$), and the values for Au-198 sources. This is considered good agreement, as error in experimental measurements and source strengths would probably introduce errors of 10 to 15 percent. This can be seen by comparing the Co-60 data of Green,[6] Eisenhauer,[8] and Terrell[9] for $L_1/W \sim 3.5$.

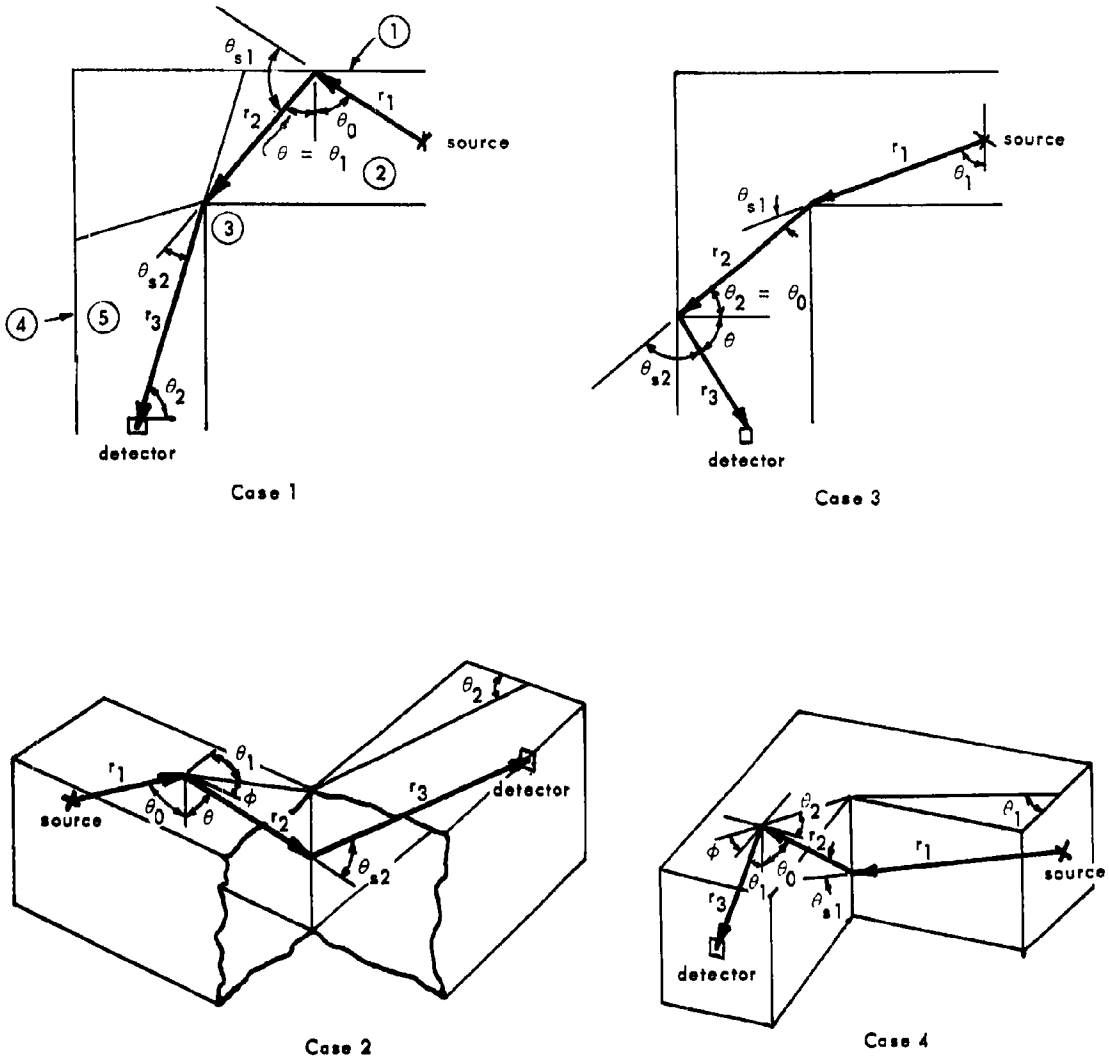

Figure 10. Geometry for multiple corner inscattering with scattering surface in the first leg (Cases 1 and 2) and in the second leg (Cases 3 and 4). Areas 2 and 5 shown in Case 1 are either ceiling or floor.

The larger error for the 12-inch duct with the Cs-137 source is evidently due to an overestimation of the corner lip effect. The use of the energy-absorption coefficient to obtain the mean free path is an overestimation that might become important in small ducts at lower incident gamma-ray energies. Also, since the energy-absorption coefficient is used, there is some double counting of gamma rays from A_5, A_6, A_7, and A_8 by including these areas in the geometry for the multiple corner lip inscattering program.

The fact that the calculations are more in error for very short first legs can be attributed to the assumptions going into the calculations; mainly those simplifying the areas in the multiple scattering program, and the assumption that the gamma rays impinging on the corner lip are parallel.

The discrepancy for Au-198 is more difficult to explain on the basis of the calculations. The fact that there is something peculiar about the Au-198 measurements can be seen from Figure 11.

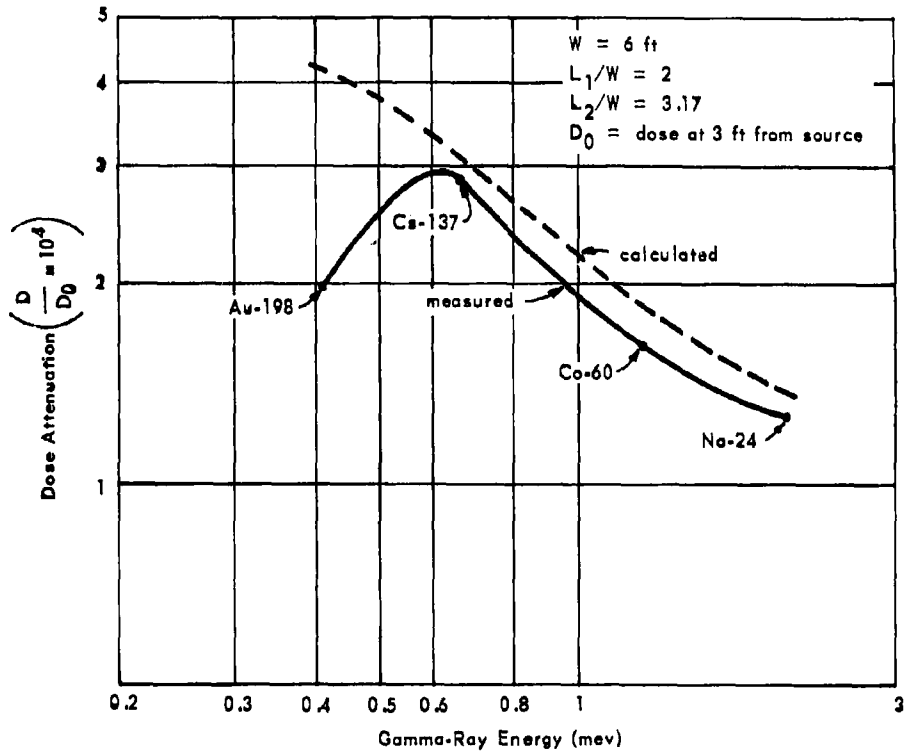

Figure 11. Variation of dose attenuation with energy for a given duct.

This figure is essentially the graph of experimentally determined attenuation factors in a 6-foot-square duct, with $L_1/W = 2$ and $L_2/W = 3.17$, versus gamma-ray energy. The points for Na-24 and Au-198 were obtained by interpolation of Terrell's data. The point for Au-198 is much lower than one would expect from the trend of the curve. The peculiarity of this point could be due to natural phenomena, or to error in the measurements. More experimental measurements of Au-198 should be made.

Tables II through V indicate the general magnitudes of the many contributing sources of scattered radiation in a duct. The contributions from all of the scattering sources considered in these calculations have been listed in Tables II and III for Co-60 and Tables IV and V for Cs-137, both for a small and a large duct.

The dose-rate contributions calculated for multiple corner lip scattering are very large, especially for small ducts. That the contribution from the corner lip is large in actuality can be seen from Figure 12.

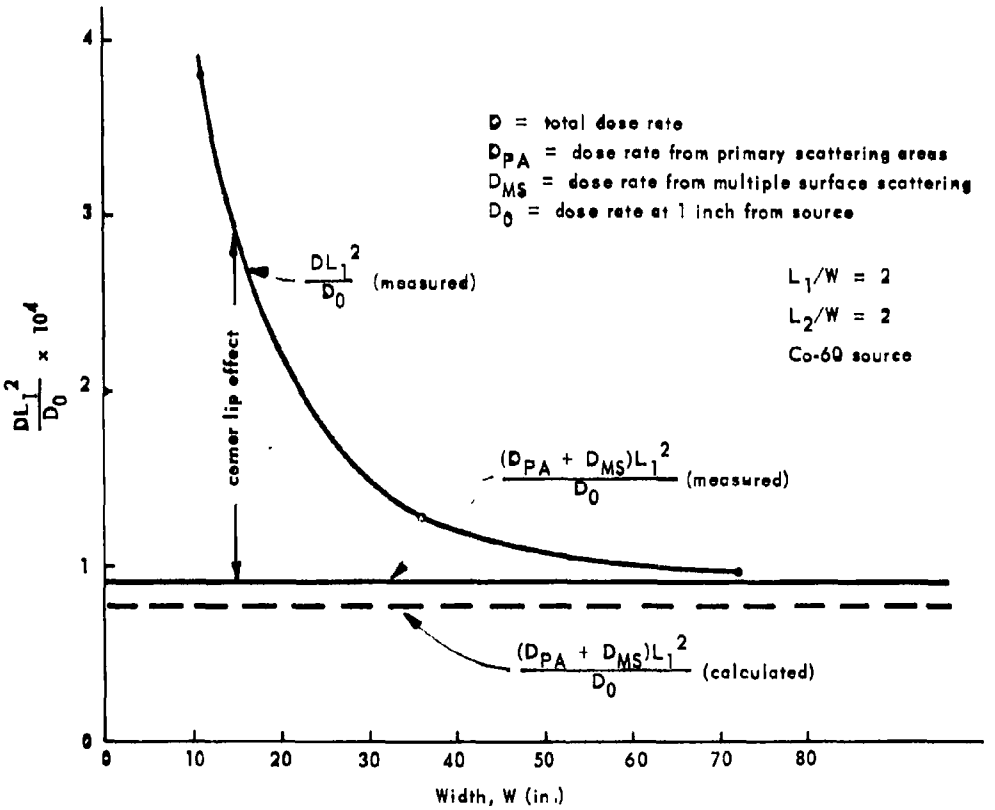

Figure 12. Variation of corner lip effect with width of duct.

In this figure the attenuation coefficient, DL_1^2/D_0, for $L_1/W = L_2/W = 2$ is plotted versus W. Also plotted in this figure is the calculated $(D_{PA} + D_{MS})L_1^2/D_0$, where D_{PA} is the dose from the primary scattering areas and D_{MS} is the dose from multiple surface scattering. Since $(D_{PA} + D_{MS})/D_0$ scales as $1/L_1^2$, the calculated $(D_{PA} + D_{MS})L_1^2/D_0$ is constant on the graph, and since the only assumption is that scattered gamma rays enter and exit at the same point, one would expect that the physical values for $(D_{PA} + D_{MS})L_1^2/D_0$ would also plot as a constant if they could be found. Since the corner lip effect decreases with W (about as 1/W), the experimental DL_1^2/D_0 does appear to asymptotically approach a constant, which is drawn on the figure. This constant is therefore labeled the experimental $(D_{PA} + D_{MS})L_1^2/D_0$, and any dose over this constant is due to the corner lip effect. As can be seen, the corner lip effects are by far the major contributors for small ducts.

The multiple surface scattering also gives a large contribution. As can be seen in the breakdown of multiple scattering contributors, this is due to 24 small contributors adding up to a sizable value, rather than to a few large contributors.

CONCLUSION

In summary, these programs appear to compute the dose rates in ducts through concrete with sufficient accuracy to assist in entranceway design. The calculations also point the way to fruitful experimentation, such as resolving the Au-198 anomaly and determining the actual corner lip effect in small ducts.

Table I. Comparison of Calculated and Measured Dose Rates

Data Source	Gamma-Ray Source	W	L_1/W	L_2/W	Dose Rate (mr/hr)		% Difference[1]
					Calculated	Measured	
Green[6]	0.34c Co-60	11 in.	1.90	1.65	87.3	125	-30
				2.06	44.5	61	-27
				2.46	27.1	30.5	-11
				3.68	8.46	7.31	+16
			3.58	2.06	6.17	7.3	-15
				2.86	2.61	2.7	-3
				3.68	1.30	1.3	0
Eisenhauer[8]	0.6c Co-60	11.1 in.	3.54	1.73	17.4	15.6	+11
				2.79	4.94	3.7	+33
				3.51	2.65	2.02	+31
Terrell[9]	55c Co-60	12 in.	3.50	2.0	916	852	+8
				3.0	317	243	+30
				4.0	140	110	+28
Chapman[7]	2.4c Co-60	3 ft	2.0	1.67	20.6	17.5	+18
				2.0	12.6	12.1	+4
				2.34	8.35	7.1	+18
			2.5	1.50	14.5	13.5	+7
				1.83	8.42	9.1	-8
				2.0	6.70	6.4	+5
				2.5	3.79	3.7	+2
Terrell[10]	3.67c Co-60	6 ft	1.33	1.83	15.4	11.8	+31
				2.50	6.56	4.75	+38
				3.17	3.47	2.42	+43
			1.66	1.83	7.85	7.30	+8
				2.50	3.46	2.73	+27
				3.17	1.85	1.39	+33
			2.0	1.83	4.71	4.56	+3
				2.50	2.12	1.79	+18
				3.17	1.14	0.935	+21
Terrell[9]	80c Cs-137	12 in.	3.5	2.0	606	430	+41
				3.0	208	132	+58
				4.0	90	90	+41
		6 ft	2.17	1.83	36.5	35.5	+3
				2.33	19.7	19.6	0
	1.52c Cs-137	6 ft	2.9	1.83	0.858	0.714	+20
				3.17	0.207	0.186	+11
Terrell[11]	8.1c Au-198	6 ft	1.66	1.83	6.90	3.22	+114
				2.50	3.09	1.37	+126
				3.17	1.60	0.738	+121
			2.17	1.83	3.41	1.66	+105
				2.50	1.54	0.714	+116
				3.17	0.818	0.370	+126
	4.2c Na-24	6 ft	1.66	1.83	8.77[2]	6.78	+29
				2.50	3.84	2.80	+37
				3.17	2.05	1.50	+37
			2.17	1.83	4.17	3.64	+15
				2.50	1.88	1.67	+13
				3.17	1.02	0.912	+11
			2.84	1.83	2.02	1.94	+9
				2.50	0.931	0.828	+12
				3.17	0.475	0.462	+3

1/ % Difference = (measured - calculated/measured) 100.

2/ The values for Na-24 are the sum of the values obtained using initial gamma-ray energies of 1.37 mev and 2.75 mev.

Table II. Comparison of Scattering Source Contributions in a 12-Inch Duct: $L_1/W = 3.5$, $L_2/W = 3$; Co-60 Source

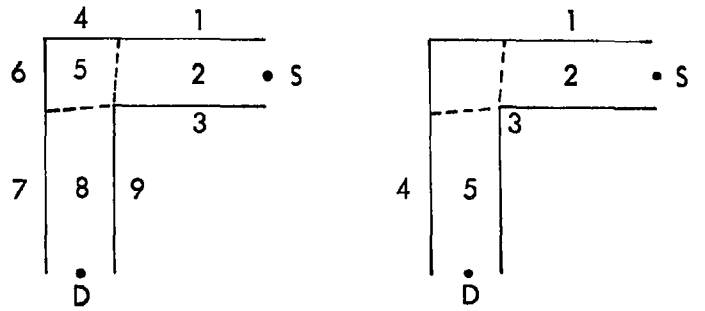

Scattering Source	% of Total
A_1	6.5
A_2	7.3
$A_3 + A_4$	11.4
A_5	1.7
A_6	1.8
A_7	0.6
A_8	2.1
Single corner lip inscatter	3.8
Multiple surface scatter	19.0
Multiple corner lip scatter	45.7
Total	99.9

Breakdown of Multiple Scatter Contribution	
Scattering Combination	% of Multiple Scatter Contribution
1-5	6.9
1-6	3.3
1-7	4.0
2-4	7.9
2-5	6.5
2-6	6.0
3-4	4.6
3-5	5.2
3-6	2.6
4-5	2.5
4-6	2.9
4-7	2.4
4-8	4.2
4-9	1.6
5-4	3.0
5-5	0.7
5-6	2.6
5-7	5.9
5-8	5.3
5-9	3.9
6-4	3.7
6-5	3.2
6-8	7.1
6-9	4.1
Total	100.1

Breakdown of Multiple Corner Lip Contribution	
Scattering Combination	% of Multiple Corner Contribution
1-3	5.6
2-3	4.5
3-4	34.8
3-5	55.0
Total	99.9

Table III. Comparison of Scattering Source Contributions in a 6-Foot Duct: $L_1/W = 2$, $L_2/W = 2.5$; Co-60 Source

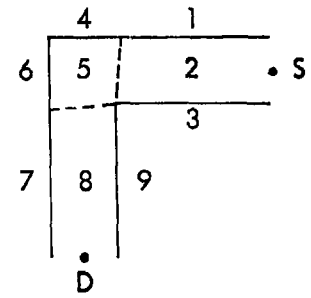

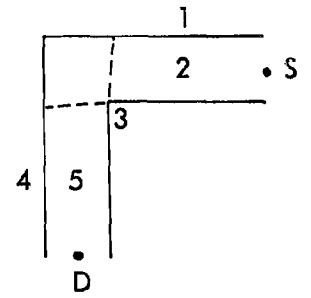

Scattering Source	% of Total
A_1	12.8
A_2	11.2
$A_3 + A_4$	23.5
A_5	0.8
A_6	1.0
A_7	0.3
A_8	1.7
Single corner lip inscatter	3.8
Multiple surface scatter	27.8
Multiple corner lip inscatter	16.9
Total	99.8

Breakdown of Multiple Scatter Contribution	
Scattering Combination	% of Multiple Scatter Contribution
1-5	6.0
1-6	2.3
1-7	5.9
2-4	6.6
2-5	5.5
2-6	4.4
3-4	3.1
3-5	4.4
3-6	2.2
4-5	3.6
4-6	3.8
4-7	2.6
4-8	5.0
4-9	2.1
5-4	3.9
5-5	1.2
5-6	3.9
5-7	6.6
5-8	6.8
5-9	5.0
6-4	2.9
6-5	3.1
6-8	6.1
6-9	3.2
Total	100.2

Breakdown of Multiple Corner Lip Contribution	
Scattering Combination	% of Multiple Corner Contribution
1-3	9.0
2-3	8.7
3-4	32.5
3-5	49.8
Total	100.0

Table IV. Comparison of Scattering Source Contributions in a 12-Inch Duct: $L_1/W = 3.5$, $L_2/W = 3$; Cs-137 Source

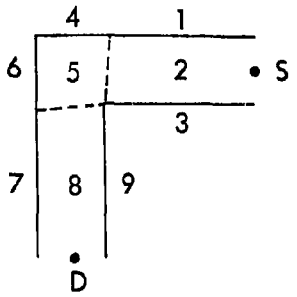

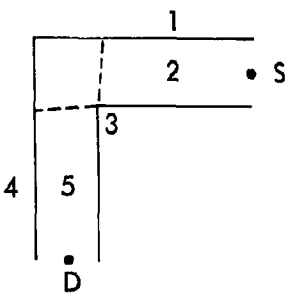

Scattering Source	% of Total
A_1	6.1
A_2	7.0
$A_3 + A_4$	10.5
A_5	1.6
A_6	1.5
A_7	0.5
A_8	1.8
Single corner lip inscatter	4.1
Multiple surface scatter	17.9
Multiple corner lip inscatter	49.0
Total	100.0

Breakdown of Multiple Scatter Contribution	
Scattering Combination	% of Multiple Scatter Contribution
1-5	6.1
1-6	2.8
1-7	3.9
2-4	7.4
2-5	6.4
2-6	5.3
3-4	4.8
3-5	5.0
3-6	2.4
4-5	2.6
4-6	2.7
4-7	2.3
4-8	4.2
4-9	1.7
5-4	3.4
5-5	0.8
5-6	2.7
5-7	5.6
5-8	5.5
5-9	4.2
6-4	4.4
6-5	3.8
6-8	7.4
6-9	4.7
Total	100.1

Breakdown of Multiple Corner Lip Contribution	
Scattering Combination	% of Multiple Corner Contribution
1-3	5.1
2-3	4.2
3-4	34.8
3-5	55.8
Total	99.9

Table V. Comparison of Scattering Source Contributions in a 6-Foot Duct: $L_1/W = 2$, $L_2/W = 2.5$; Cs-137 Source

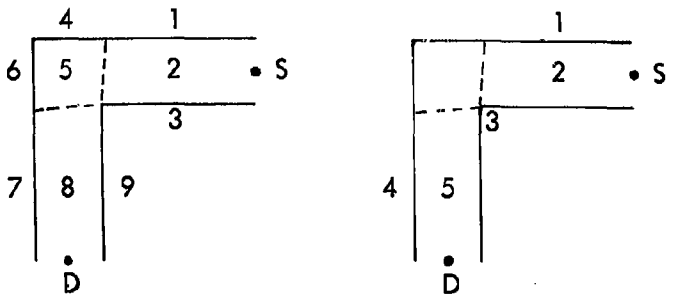

Scattering Source	% of Total
A_1	12.7
A_2	11.0
$A_3 + A_4$	22.0
A_5	0.9
A_6	0.9
A_7	0.3
A_8	1.4
Single corner lip inscatter	3.9
Multiple surface scatter	28.5
Multiple corner lip inscatter	18.4
Total	100.0

Breakdown of Multiple Scatter Contribution	
Scattering Combination	% of Multiple Scatter Contribution
1-5	5.7
1-6	2.2
1-7	5.7
2-4	6.6
2-5	5.5
2-6	4.3
3-4	3.2
3-5	4.5
3-6	2.1
4-5	3.6
4-6	3.4
4-7	2.5
4-8	4.9
4-9	2.1
5-4	4.2
5-5	1.3
5-6	3.8
5-7	6.1
5-8	6.8
5-9	5.2
6-4	3.3
6-5	3.5
6-8	6.1
6-9	3.5
Total	100.1

Breakdown of Multiple Corner Lip Contribution	
Scattering Combination	% of Multiple Corner Contribution
1-3	8.9
2-3	8.3
3-4	31.1
3-5	51.7
Total	100.0

REFERENCES

1. NCEL Technical Note N-383, Attenuation of Gamma Radiation Through Two-Legged Rectangular Ducts — An Analytical Approach, by J. C. LeDoux and A. B. Chilton. Port Hueneme, California, 20 January 1961.

2. Technical Operations, Inc. Report TO-B 61-39, Monte Carlo Calculations on the Reflection and Transmission of Scattered Gamma Radiation (revised), by D. J. Raso. Burlington, Massachusetts, May 1962.

3. NCEL Technical Report R-228, A Semiempirical Formula for Differential Dose Albedo of Gamma Rays on Concrete, by A. B. Chilton and C. M. Huddleston. Port Hueneme, California, 16 November 1962.

4. NCEL Technical Note N-469, Some Applications of a Semiempirical Formula for Differential Dose Albedo for Gamma Rays on Concrete, by W. C. Ingold. Port Hueneme, California, 30 November 1962.

5. Rockwell, T., III, editor. Reactor Shielding Design Manual. McGraw-Hill, New York, 1956.

6. NCEL Technical Report R-195, Attenuation of Gamma Radiation in a Two-Legged 11-Inch Rectangular Duct, by D. W. Green. Port Hueneme, California, 2 May 1962.

7. NCEL Technical Note N-443, Gamma Dose Rates and Energy Spectra in a 3-Foot Square Duct, by J. M. Chapman. Port Hueneme, California, 29 June 1962.

8. National Bureau of Standards. Technical Note 74, Scattering of Cobalt-60 Gamma Radiation in Air Ducts, by C. Eisenhauer. Washington, D. C., 1960.

9. Armour Research Foundation. Report ARF 1158-A02-7, Radiation Streaming in Shelter Entranceways, by C. W. Terrell, et al. Chicago, 1962.

10. Armour Research Foundation. Report ARF 1158-12, Radiation Streaming in Shelter Entranceways, by C. W. Terrell, et al. Chicago, 1960.

11. Armour Research Foundation. Report ARF 1158-A01-5, Radiation Streaming in Shelter Entranceways, by C. W. Terrell, et al. Chicago, 1961.

DISTRIBUTION LIST

SNDL Code	No. of Activities	Total Copies	
	1	10	Chief, Bureau of Yards and Docks (Code 42)
23A	1	1	Naval Forces Commanders (Taiwan only)
39B	2	4	Construction Battalions
39D	10	10	Mobile Construction Battalions
39E	3	3	Amphibious Construction Battalions
39F	1	2	Construction Battalion Base Units
A2A	1	1	Chief of Naval Research - Only
A3	2	2	Chief of Naval Operation (OP-07, OP-04)
A5	5	5	Bureaus
B3	2	2	Colleges
E4	1	2	Laboratory ONR (Washington, D. C. only)
E5	1	1	Research Office ONR (Pasadena only)
E16	1	1	Training Device Center
F9	7	7	Station - CNO (Boston; Key West; San Juan; Long Beach; San Diego; Treasure Island; and Rodman, C. Z. only)
F17	6	6	Communication Station (San Juan; San Francisco; Pearl Harbor; Adak, Alaska; and Guam only)
F41	1	1	Security Station
F42	1	1	Radio Station (Oso and Cheltanham only)
F48	1	1	Security Group Activities (Winter Harbor only)
H3	8	8	Hospital (Chelsea; St. Albans, Portsmouth, Va; Beaufort; Great Lakes; San Diego; Oakland; and Camp Pendleton only)
H6	1	1	Medical Center
J1	2	2	Administration Command and Unit - BuPers (Great Lakes and San Diego only)
J3	1	1	U. S. Fleet Anti-Air Warfare Training Center (Virginia Beach only)
J4	2	2	Amphibious Bases
J19	1	1	Receiving Station (Brooklyn only)
J34	1	1	Station - BuPers (Washington, D. C. only)
J46	1	1	Personnel Center
J48	1	1	Construction Training Unit
J60	1	1	School Academy
J65	1	1	School CEC Officers
J84	1	1	School Postgraduate
J90	1	1	School Supply Corps

DISTRIBUTION LIST (Cont'd)

SNDL Code	No. of Activities	Total Copies	
J95	1	1	School War College
J99	1	1	Communication Training Center
L1	11	11	Shipyards
L7	4	4	Laboratory - BuShips (New London; Panama City; Carderock; and Annapolis only)
L26	5	5	Naval Facilities - BuShips (Antigua; Turks Island; Barbados; San Salvador; and Eleuthera only)
L30	1	1	Submarine Base (Groton, Conn. only)
L32	2	2	Naval Support Activities (London and Naples only)
L42	2	2	Fleet Activities - BuShips
M27	4	4	Supply Center
M28	6	6	Supply Depot (except Guantanamo Bay; Subic Bay; and Yokosuka)
M61	2	2	Aviation Supply Office
N1	6	18	BuDocks Director, Overseas Division
N2	9	27	Public Works Offices
N5	3	9	Construction Battalion Center
N6	5	5	Construction Officer-in-Charge
N7	1	1	Construction Resident-Officer-in-Charge
N9	6	12	Public Works Center
N14	1	1	Housing Activity
R9	2	2	Recruit Depots
R10	2	2	Supply Installations (Albany and Barstow only)
R20	1	1	Marine Corps Schools (Quantico)
R64	3	3	Marine Corps Base
R66	1	1	Marine Corps Camp Detachment (Tengan only)
W1A1	6	6	Air Station
W1A2	35	35	Air Station
W1B	8	8	Air Station Auxiliary
W1C	4	4	Air Facility (Phoenix; Monterey; Oppama; Naha; and Naples only)
W1E	6	6	Marine Corps Air Station (except Quantico)
W1H	9	9	Station - BuWeps (except Rota)
	1	1	Deputy Chief of Staff, Research and Development, Headquarters, U. S. Marine Corps, Washington, D. C.
	1	1	President, Marine Corps Equipment Board, Marine Corps School, Quantico, Va.
	1	2	Library of Congress, Washington, D. C.
	1	1	U. S. Naval Research Laboratory, Chemistry Division, Washington, D. C.
	1	1	Deputy Chief of Staff, Research and Development Headquarters, U. S. Marine Corps, Washington, D. C.

DISTRIBUTION LIST (Cont'd)

No. of Activities	Total Copies	
1	1	Chief of Staff, U. S. Army, Chief of Research and Development, Department of the Army, Washington, D. C.
1	1	Office of the Chief of Engineers, Assistant Chief of Engineering for Civil Works, Department of the Army, Washington, D. C.
1	1	Chief of Engineers, Department of the Army, Washington, D. C., Attn: Engineering Research and Development Division
1	1	Chief of Engineers, Department of the Army, Washington, D. C., Attn: ENGCW-OE
1	1	Director, U. S. Army Engineer Research and Development Laboratories, Fort Belvoir, Va., Attn: Information Resources Branch
1	1	ASD (ASNXRR), Wright-Patterson Air Force Base, Ohio
1	3	Headquarters, U. S. Air Force, Directorate of Civil Engineering, Washington, D. C., Attn: AFOCE-ES
1	1	Commanding Officer, U. S. Naval Construction Battalion Center, Port Hueneme, Calif., Attn: Materiel Dept., Code 140
1	1	Deputy Chief of Staff, Development, Director of Research and Development, Department of the Air Force, Washington, D. C.
1	1	Director, National Bureau of Standards, Department of Commerce, Connecticut Avenue, Washington, D. C.
1	2	Office of the Director, U. S. Coast and Geodetic Survey, Washington, D. C.
1	20	Defense Documentation Center, Building 5, Cameron Station, Alexandria, Va.
1	2	Director of Defense Research and Engineering, Department of Defense, Washington, D. C.
1	2	Director, Division of Plans and Policies, Headquarters, U. S. Marine Corps, Washington, D. C.
1	2	Director, Bureau of Reclamation, Washington, D. C.
1	1	Facilities Officer, Code 108, Office of Naval Research, Washington, D. C.
1	1	Federal Aviation Agency, Office of Management Services, Administrative Services Division, Washington, D. C., Attn: Library Branch
1	2	Commander Naval Beach Group TWO, U. S. Naval Amphibious Base, Little Creek, Norfolk, Va.
1	1	Commander, Pacific Missile Range, Technical Documentation Section, P. O. Box 10, Point Mugu, Calif., Attn: 4332
1	1	Air Force Cambridge Research Center, Hanscom Field, Bedford, Mass.
1	1	Directorate of Research, Air Force Special Weapons Center, Kirtland Air Force Base, N. M.
1	1	Sandia Corporation, Box 5800, Albuquerque, N. M., Attn: Classified Document Division
1	1	Director, Engineering Research Institute, University of Michigan, Ann Arbor, Mich.
1	4	U. S. Army Material Command, Washington, D. C.
1	1	Dr. H. E. Stanton, Physics Division, Argonne National Laboratory, Argonne, Ill.
1	1	Mr. John H. Hubbell, National Bureau of Standards, Washington, D. C.
1	1	Professor D. W. Green, 1668 Maple Avenue, Galesburg, Ill.
1	1	Rivers and Harbor Library, Princeton University, Princeton, N. J.

U. S. Naval Civil Engineering Laboratory
Technical Report R-264
COMPUTER CALCULATION OF DOSE RATES IN TWO-LEGGED DUCTS USING THE ALBEDO CONCEPT, by J. M. Chapman
27 p. illus 24 Oct 63 UNCLASSIFIED

Computer calculations based on the differential dose albedo are made of gamma-ray rates in two-legged ducts, and the results are compared with experimental data.

1. Shelters — Dose rates Radiation streaming
I. Chapman, J. M.
II. Y-F011-05-329

U. S. Naval Civil Engineering Laboratory
Technical Report R-264
COMPUTER CALCULATION OF DOSE RATES IN TWO-LEGGED DUCTS USING THE ALBEDO CONCEPT, by J. M. Chapman
27 p. illus 24 Oct 63 UNCLASSIFIED

Computer calculations based on the differential dose albedo are made of gamma-ray rates in two-legged ducts, and the results are compared with experimental data.

1. Shelters — Dose rates Radiation streaming
I. Chapman, J. M.
II. Y-F011-05-329

U. S. Naval Civil Engineering Laboratory
Technical Report R-264
COMPUTER CALCULATION OF DOSE RATES IN TWO-LEGGED DUCTS USING THE ALBEDO CONCEPT, by J. M. Chapman
27 p. illus 24 Oct 63 UNCLASSIFIED

Computer calculations based on the differential dose albedo are made of gamma-ray rates in two-legged ducts, and the results are compared with experimental data.

1. Shelters — Dose rates Radiation streaming
I. Chapman, J. M.
II. Y-F011-05-329

U. S. Naval Civil Engineering Laboratory
Technical Report R-264
COMPUTER CALCULATION OF DOSE RATES IN TWO-LEGGED DUCTS USING THE ALBEDO CONCEPT, by J. M. Chapman
27 p. illus 24 Oct 63 UNCLASSIFIED

Computer calculations based on the differential dose albedo are made of gamma-ray rates in two-legged ducts, and the results are compared with experimental data.

1. Shelters — Dose rates Radiation streaming
I. Chapman, J. M.
II. Y-F011-05-329